Theor Chem Acc (2001) 106:2–9
DOI 10.1007/s002140000216

Theoretical
Chemistry Accounts

*Regular article*

# How accurate can molecular dynamics/linear response and Poisson–Boltzmann/solvent accessible surface calculations be for predicting relative binding affinities? Acetylcholinesterase huprine inhibitors as a test case

**X. Barril[1], J. L. Gelpí[2], J. M. López[1], M. Orozco[2], F. J. Luque[1]**

[1] Departament de Físico-Química, Facultat de Farmàcia, Universitat de Barcelona, Av. Diagonal s/n, 08028 Barcelona, Spain
e-mail: javier@far1.far.ub.es
[2] Departament de Bioquímica, Facultat de Química, Universitat de Barcelona, Av. Martí i Franqués 1, 08028 Barcelona, Spain
e-mail: modesto@luz.bq.ub.es

Received: 2 August 2000 / Accepted: 8 September 2000 / Published online: 21 December 2000


**Abstract.** This study examines the accuracy of molecular dynamics-linear response (MD/LR) and Poisson–Boltzmann/solvent accessible surface (PB/SAS) calculations to predict relative binding affinities. A series of acetylcholinesterase (AChE) huprine inhibitors has been chosen as a test system owing to the availability of free-energy (thermodynamic integration) calculations. The results obtained with the MD/LR approach point out a clear relationship between the experimental affinity and the electrostatic interaction energy alone for a subset of huprines, but the suitability of the MD/LR approach to predict the binding affinity of the whole series of compounds is limited. On the other hand, PB/SAS calculations show a marked dependence on both the computational protocol and the nature of the inhibitor–enzyme complex.

**Key words:** Free-energy calculations – Linear response approximation – Poisson–Boltzmann/solvent accessible surface calculations – Prediction of binding affinities – Acetylcholinesterase inhibitors

## 1 Introduction

Acetylcholinesterase (AChE) is an active target for drug development owing to the cholinergic deficit associated with Alzheimer's disease [1, 2]. Tacrine (Cognex) was the first inhibitor approved for the palliative treatment of Alzheimer's disease senile dementia, though its clinical efficacy is limited owing to undesirable side effects, especially hepatotoxicity [3]. Research efforts have concentrated on analogues of tacrine [4], huperzine [5] and derivatives of physostigmine [6], *N*-benzylpiperidines [7], and xanthones [8], leading to the discovery of the recently marketed donepezil (Aricept) [9] and rivagstimine (Exelon) [10]. The synthesis, in vitro pharmacology and molecular modeling of a series of tacrine–huperzine A hybrids (huprines; Fig. 1) as AChE inhibitors have been reported recently [11, 12, 13]. The most potent compound has an inhibition constant ($K_I$) for human AChE of 26 pM, which means an affinity around 1200 times higher than that of tacrine [14, 15], making these compounds valuable candidates for the palliative treatment of Alzheimer's disease.

Molecular modeling of the interaction of huprines with *Torpedo californica* AChE suggested that they behave as true tacrine–huperzine A hybrids [13, 16], since the 4-aminoquinoline and bicyclo[3.3.1]nonadiene subunits roughly occupy the positions of the corresponding moieties in tacrine and (−)-huperzine A, as determined from their crystallographic complexes with AChE [17, 18]. The huprine lies at the bottom (near 20 Å from the surface) of the channel leading to the enzyme active site, stacked between the rings of Trp84 and Phe330. The $NH_2$ group is linked to different residues, such as Asp72, Ser81, Tyr121 and Ser122, through water-mediated bridges. The NH group is hydrogen-bonded to the carbonyl oxygen of His440. Finally, the bicyclo[3.3.1]nonadiene subunit fits into a cavity formed by aromatic residues, such as Phe290 and Phe331. This putative binding model has recently been validated from the crystallographic structure of the *T. californica* AChE complexes with the (−)-enantiomer of the 9-ethyl,3-chloro huprine derivative.

Free-energy (thermodynamic integration, TI) calculations carried out using this binding model reflected successfully the differences in inhibitory activity for a small series of selected huprines [15, 16]. These calcula-

*Correspondence to*: F. J. Luque

Contribution to the Symposium Proceedings of Computational Biophysics 2000

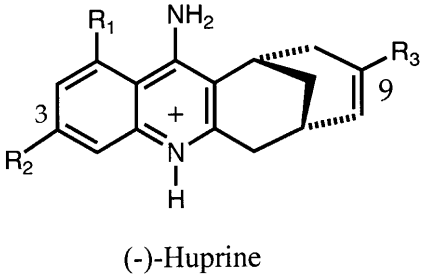


(-)-Huprine

**Fig. 1.** Schematic representation of the acetylcholinesterase inhibitors tacrine and the (−)-enantiomer of huprine

tions give typically good estimates of the differences in binding free energies for related compounds [19]; however, they are computationally very demanding, since only one pair of inhibitors can be compared in a single calculation, which may require several days to complete. Obviously, this severely limits their application in drug discovery and has stimulated the development of approximate methods to rank efficiently large series of inhibitors with regard to the binding free energy to a common receptor [20, 21, 22, 23, 24, 25].

In this study we explore the accuracy of two approximate methods to predict the relative binding affinities of huprines for AChE. The first method relies on the extended linear response (LR) approximation [20, 21, 22] using the ensemble of configurations collected from molecular dynamics (MD) simulations. The second approach is based on the calculation of binding affinities from Poisson–Boltzmann (PB) calculations [23] supplemented with terms related to solvent accessibility (SA). Discussion is made of the capabilities of these approximate techniques to predict the inhibitory activity for the series of huprine compounds.

## 2 Methods

### *2.1 AChE inhibitors*

A total of 14 huprine compounds were considered in the study, including derivatives substituted at positions 1, 3 and 9 (Fig. 1, Table 1). In all cases the levorotatory enantiomer of the huprine derivative was found to be more potent than the dextrorotatory one [15, 16]. Since the experimental inhibitory activity (expressed as IC50 values) of the active enantiomer is available only for a few compounds, the possibility to perform a reliable comparison between methods is limited. This forced us to use the inhibitory data reported for the racemic mixture, which exhibits a linear relationship with the inhibitory potency of the (−)-enantiomer ($IC50_{(-)} = -1.70 + 0.75\ IC50_{rac}$; $r_P > 0.99$; $p < 0.001$) for those compounds where the two activity measurements are available. Since the substrate concentration in the in vitro assays (performed at 298 K) was the same for all the huprines, the experimental differences in binding free energy were derived from the competitive inhibition equation $IC50 = K_I(1 + [S]/K_M)$, where $K_M$ and $K_I$ are Michaelis and enzyme–inhibitor dissociation constants.

### *2.2 MD/LR calculations*

In the MD/LR approach both the ligand and the environment (protein, solvent) are described at the discrete level and the binding free energy is estimated assuming a linear response for the nonbonded (electrostatic and van der Waals) interaction energy terms, as noted in Eq. (1). The terms $U_{bound}$ and $U_{unbound}$ refer to the bound and unbound states of the inhibitor and the subindexes "vdW" and "ele" denote that the interaction energy (averaged for the ensemble of configurations sampled in the MD simulation) of the inhibitor with its environment involves either Lennard-Jones or electrostatic contributions. Though a value of 0.5 can be used as a first guess, it has been argued that this parameter can vary depending on the nature of the inhibitor and the simulation protocol [22]. Accordingly, the coefficients $\alpha$ and $\beta$ are typically determined empirically to obtain the best fit to the experimental observable. A third term is sometimes included to account for the cost of creating a cavity in the solvent, which is made proportional to the change in the solvent accessible surface (SAS) of the inhibitor upon binding (Eq. 2) or it is simply replaced with a constant (Eq. 3) [21]. The corresponding coefficients $\gamma$ and $\delta$ are typically determined by fitting to the experimental data.

$$\Delta G_{binding} = \alpha(\langle U_{bound}\rangle - \langle U_{unbound}\rangle)_{vdW} + \beta(\langle U_{bound}\rangle - \langle U_{unbound}\rangle)_{ele} \quad (1)$$

$$\Delta G_{binding} = \alpha(\langle U_{bound}\rangle - \langle U_{unbound}\rangle)_{vdw} + \beta(\langle U_{bound}\rangle - \langle U_{unbound}\rangle)_{ele} + \gamma(\langle SAS_{bound}\rangle - \langle SAS_{unbound}\rangle) \quad (2)$$

$$\Delta G_{binding} = \alpha(\langle U_{bound}\rangle - \langle U_{unbound}\rangle)_{vdW} + \beta(\langle U_{bound}\rangle - \langle U_{unbound}\rangle)_{ele} + \delta \quad (3)$$

### *2.3 MD simulations*

For the bound inhibitor, the simulation system consisted of the *T. californica* AChE complexed to the huprine and a sphere of 25 Å of TIP3P water molecules [26] centered at the inhibitor. In order to compare the predicted relative binding free energies with the experimental data, the Phe330 residue in the *T. californica* enzyme was changed to Tyr, which is the corresponding residue in bovine

**Table 1.** Acetylcholinesterase (*AChE*) inhibitors considered in the study and their IC50 inhibitory values (nM) for bovine erythrocyte AChE determined for the racemic mixture and the (−)-enantiomer determined from inhibition of bovine erythrocyte AChE (standard error in *parentheses*). Data taken from Refs. [13, 15]

| Compound | $R_1$ | $R_2$ | $R_3$ | $IC50_{rac}$ | $IC50_{(-)}$ |
|---|---|---|---|---|---|
| H1 | H | H | Methyl | 65 ± 15 | 47.1 ± 6.3 |
| H2 | H | Methyl | Methyl | 12.4 ± 2.3 | |
| H3 | F | H | Methyl | 31.4 ± 0.8 | |
| H4 | H | F | Methyl | 8.5 ± 1.8 | 3.5 ± 0.8 |
| H5 | H | Cl | Methyl | 4.2 ± 0.3 | 1.2 ± 0.1 |
| H6 | H | H | Ethyl | 38.5 ± 4.0 | 27.4 ± 3.1 |
| H7 | Methyl | H | Ethyl | 29.8 ± 6.2 | |
| H8 | H | Methyl | Ethyl | 12.0 ± 2.2 | 4.5 ± 0.8 |
| H9 | Methyl | Methyl | Ethyl | 3.6 ± 0.2 | |
| H10 | F | H | Ethyl | 46.4 ± 8.5 | |
| H11 | H | F | Ethyl | 7.4 ± 1.5 | 6.7 ± 1.0 |
| H12 | Cl | H | Ethyl | 16.2 ± 4.4 | |
| H13 | H | Cl | Ethyl | 2.8 ± 0.8 | 1.3 ± 0.3 |
| H14 | Cl | Cl | Ethyl | 39.6 ± 11.6 | |

AChE. Such a mutation is the only relevant difference concerning the residues directly involved in the binding pocket between *T. californica* and human enzymes.

The enzyme was modeled in its physiological active form with neutral His440 and deprotonated Glu327, which together with Ser200 form the catalytic triad. The standard ionization state at neutral pH was considered for the rest of the ionizable residues with the exception of Asp392 and Glu443, which were neutral, and His471, which was protonated, in accordance with previous numerical titration studies [27]. The geometry of the inhibitor was fully optimized at the Hartree–Fock (HF) level with the 6-31G(d) basis set [28] using the Gaussian 94 program [29]. According to the acidity of H16 ($pK_a = 8.9$) [14], the protonated species was considered in the calculations.

The starting structure was taken from the equilibrated system obtained in our MD simulations (see Refs. [15, 16] for detailed explanations). Those huprines not previously examined in our studies [15, 16] were positioned in the enzyme to fit the set of interactions involved in the binding mode. The final model system was partitioned into a mobile and a rigid region. The former included the inhibitor, all the protein residues containing at least one atom within 14 Å from the inhibitor and all the water molecules, while the rest of atoms defined the rigid part. Both mobile and rigid regions were allowed to relax during the equilibration of the system, but only the mobile region was free to move during a 0.5-ns MD simulation at 298 K.

The AMBER-95 all-atom force field [30] was used for the entire system but the hybrid compound. The charge distribution of the drug was determined from fitting to the HF/6-31G(d) electrostatic potential using the RESP procedure [31], and the van der Waals parameters were taken from those defined for related atoms in the AMBER-95 force field. SHAKE [32] was used to maintain all the bonds at their equilibrium distances, which allowed an integration time step of 2 fs. A cutoff of 11 Å was used for nonbonded interactions. The trajectory was stored every 1 ps for subsequent analysis of the complexes. Averaged Lennard-Jones and electrostatic interaction energies and SAS were determined from the structures collected during the last 0.3 ns, though the values did not exhibit remarkable differences relative to those obtained from the structures acquired during the first 0.2 ns of the simulation, suggesting that the system was equilibrated. Calculations were performed using the AMBER5 computer program [33].

For the unbound inhibitor, the systems consisted of the inhibitor immersed in a cap of 25 Å centered at the inhibitor. A 10-Å cutoff distance for the nonbonded interactions was used. The rest of the simulation protocol was identical to that reported for the bound inhibitor. Again, the averaged energetic quantities determined during the last 0.3 ns of the simulation were similar to the values obtained in the first part of the simulation.

### *2.4 PB/SA method*

In this approach the difference in the binding free energy between two inhibitors was determined from the addition of electrostatic ($\Delta G_{ele}$) and nonelectrostatic ($\Delta G_{n\text{-}ele}$) contributions, as noted in Eq. (4).

$$\Delta G_{binding} = \Delta G_{ele} + \Delta G_{n\text{-}ele} \tag{4}$$

The electrostatic term in Eq. (4 ) was computed by adding the change in the desolvation free energy of both ligand ($\Delta\Delta G_{S,L}$) and receptor ($\Delta\Delta G_{S,R}$) upon binding plus the solvent-screened interaction energy between ligand and receptor ($\Delta G_{int}$), as noted in Eq. (5). The desolvation term was determined from the difference in the solvation free energy of the ligand/receptor in its own cavity [$\Delta G_{S,L}(L)$; $\Delta G_{S,R}(R)$] and in a cavity generated by removing the solvent from the region that the receptor/ligand occupies in the complex [$\Delta G_{S,L}(LR)$; ($\Delta G_{S,R}(LR)$]. The solvent-screened interaction term was determined from the products between the charges in the receptor ($q_{iR}$) placed at $\mathbf{r}_i$ and the solvent-screened potential [$V_L(\mathbf{r}_i)$] created by the charges of the ligand in the complex at positions $\mathbf{r}_i$.

$$\Delta G_{ele} = \Delta G_{int} + \Delta\Delta G_{S,L1} + \Delta\Delta G_{S,R} \tag{5}$$

The desolvation of the receptor can be assumed to be common for all the complexes between AChE and the inhibitors examined here, and the differences in the electrostatic term can be approximated as given in Eq. (6). Since this procedure only involves calculations with the charge distribution of the inhibitor, it provides a substantial saving in computer time.

$$\Delta\Delta G_{ele} = (\Delta G_{int,L1} - G_{int,L2}) + (\Delta\Delta G_{S,L1} - \Delta\Delta G_{S,L2)} \tag{6}$$

The different electrostatic contributions were determined from a finite-difference solution of the PB equation [23]. The solvent was represented as a continuum with a dielectric constant of 78.4, and the protein and the inhibitor were treated as cavities with a dielectric constant of 1 containing fixed partial charges on their atoms. The dielectric boundary was defined using a 1.4-Å probe sphere and atomic van der Waals radii taken from the AMBER-95 force field, which was also used to assign atomic charges. A grid of 1.5 Å/point was used in the PB calculations, which were carried out with the CMIP program. [36].

The nonelectrostatic term in Eq. (4 ) was determined from the addition of two contributions, as noted in Eq. (7). The first accounts for the van der Waals interaction energy between enzyme and inhibitor ($\Delta G_{vdW}$), which was computed using the van der Waals parameters in the AMBER-95 force field. The second is related to the nonelectrostatic component of the change in the solvation free energy, which was estimated from an empirical relationship with the change in the SAS of ligand ($SAS_L$)and receptor upon binding. As noted previously for the electrostatic term, this latter contribution was approximated from the change in the SAS of the ligand in its bound [$SAS_L$(L-R)] and unbound [$SAS_L$(L)] states. A value of 5.4 cal/mol/Å$^2$ was adopted for the microscopic surface tension, $\sigma$, of all parts of the surface [35].

$$\Delta G_{n\text{-}ele} = \Delta G_{vdW} + \sigma\Delta SAS_L = \Delta G_{vdW} + \sigma[SAS_L(L\text{-}R) - SAS_L(L)] \tag{7}$$

In order to avoid uncertainties due to misplacement of the inhibitor in the binding pocket, PB/SA calculations were performed for a set of 20 structures of the enzyme–inhibitor complex uniformly taken from the last 0.2 ns of the MD simulation mentioned earlier. Prior to the calculations, the complexes were energy-minimized to eliminate bad contacts (water molecules, inhibitor and residues in the mobile part were minimized in a sequential way for a total of 2000 steps; at the end, all the water molecules were removed). The relative binding free energies were determined from the difference between the average values computed for the set of 20 structures and the most favorable binding free energy obtained for each inhibitor.

## 3 Results and discussion

Let us start the investigation on the predictive power of MD/LR and PB/SA methods by firstly considering the subset formed by the huprines H1, H4, H5, H6, H11 and H13, which involve substitutions at positions 3 ($R_2$) and 9 ($R_3$). This preliminary analysis is useful since for this small series of compounds the activity of the bioactive enatiomer is known, the binding mode of this enantiomer has been characterized by molecular modeling and crystallographic studies and relative binding free energies computed from MD/TI calculations are available [15, 16].

The averaged electrostatic and van der Waals interaction energies of the inhibitor in the enzyme and in solution determined from MD/LR calculations and the corresponding SASs of the inhibitor are given in Table 2. The relative differences in electrostatic energy between bound and unbound states ($\Delta\Delta U_{ele}$) varies around 26 kcal/mol for the subset of compounds. This variation mainly stems from the interaction between inhibitor and enzyme (ranging from −164.9 to −194.0 kcal/mol), while the electrostatic energy for the

unbound inhibitor lies in a range of around 4 kcal/mol (from −75.2 to −79.3 kcal/mol). Attachment of fluorine or chlorine at position 3 (compounds H4, H5, H11 and H13; see Fig. 1 for nomenclature) makes the electrostatic interaction between inhibitor and enzyme more favorable compared to the respective unsubstituted compounds, H1 and H6. The difference in the van der Waals interaction energy between bound and unbound states ($\Delta\Delta U_{vdW}$) varies around 2 kcal/mol. Replacement of methyl by ethyl at $R_3$ favors the van der Waals interaction between inhibitor and enzyme by 1–2 kcal/mol. Finally, all the inhibitors are almost completely buried in the enzyme. Accordingly, the changes in the SAS between bound and unbound states (ΔΔSAS) of the inhibitor largely reflect the differences in the SAS of the inhibitor in solution.

The electrostatic and nonelectrostatic contributions to the binding free energy determined from PB/SA calculations are reported in Table 3. The results are given for the average contribution determined for the 20 complexes collected along the MD simulation performed for each inhibitor as well as for the bound complex leading to the highest binding affinity (see Methods). The contributions due to inhibitor desolvation ($\Delta\Delta G_{s,L}$), inhibitor–enzyme van der Waals interaction ($\Delta G_{vdW}$) and change in SAS of the inhibitor ($\sigma\Delta SAS_L$) are very similar in the two sets of results. The solvent-screened electrostatic interaction ($\Delta G_{int}$) is more negative and its range is larger for the complex showing the highest binding affinity compared to the average results. More importantly, the ordering of binding free energies differs depending on whether the average binding affinity or the highest one is considered. Thus, in the former case compounds H11 and H13 are predicted to be the most potent inhibitors, whereas in the latter case the highest inhibitory potency is predicted for H5 and H11. Moreover, compound H4 is expected to bind less tightly than H1 according to the average values, but the reverse situation is predicted from the results obtained for the structure with the highest binding affinity.

Comparison of the predicted rank of inhibitory potency with the inhibitory data is made in Table 4, which gives the relative binding free energies determined from the IC50 values for this subset of huprines. There is close similarity in the relative binding affinities derived from the IC50 data for either the bioactive enantiomer or the racemic mixture. The order of the two most active compounds (H5, H13) is, nevertheless, reversed depending on whether the data of the (−)-enantiomer or the racemic mixture is considered. Table 4 also reports the relative binding free energies determined in our previous studies from free-energy (TI) calculations [15, 16]. The TI results overestimate the differences in binding free energy compared to the experimental values; however, the rank of the compounds satisfactorily reflects the experimental ordering, as they clearly identify the compounds having low, intermediate and high affinity for the enzyme ($r_S = 0.89$).

Inspection of the separate MD/LR contributions revealed a marked dependence of the inhibitory activity with the electrostatic term, as can be seen from inspection of Fig. 2. Thus, good correlation between the relative binding free energies and the electrostatic term is found [Pearson's correlation coefficient of 0.93 and 0.96 if data derived from the (−)-enantiomer or the racemic mixture are used; see Eqs. 8 ($p < 0.005$), 9 ($p < 0.005$)]. The positive value of the coefficient ($\beta$) in Eqs. (8) and (9) implies that the binding affinity increases as the

**Table 2.** Averaged electrostatic and van der Waals interaction energies (kcal/mol) and solvent accessible surface (*SAS*) (Å$^2$) for the inhibitor complexed to the enzyme and in solution

| Compound | van der Waals | | | Electrostatic | | | SAS | | |
|---|---|---|---|---|---|---|---|---|---|
| | $U_{bound}$ | $U_{unbound}$ | $\Delta\Delta U_{vdW}$[a] | $U_{bound}$ | $U_{unbound}$ | $\Delta\Delta U_{ele}$[a] | Bound | Unbound | $\Delta\Delta SAS$[a] |
| H1 | −48.0 | −23.7 | 0.0 | −164.9 | −75.2 | 0.0 | 18.2 | 449.2 | 0.0 |
| H4 | −47.7 | −24.2 | 0.8 | −189.1 | −79.3 | −20.1 | 16.1 | 460.7 | −13.5 |
| H5 | −48.9 | −24.8 | 0.2 | −186.8 | −79.0 | −18.1 | 13.4 | 474.1 | −29.7 |
| H6 | −49.8 | −24.8 | −0.7 | −172.1 | −75.6 | −6.8 | 14.1 | 473.1 | −28.0 |
| H11 | −51.2 | −25.3 | −1.6 | −184.1 | −78.4 | −16.1 | 13.4 | 485.0 | −40.6 |
| H13 | −52.0 | −25.6 | −2.1 | −194.0 | −78.3 | −26.0 | 13.6 | 504.2 | −59.6 |

[a] Values relative to those of compound H1

**Table 3.** Electrostatic and nonelectrostatic contributions (kcal/mol) to the binding free energy determined from Poisson–Boltzmann (*PB*)/SAS calculations. Values averaged for the inhibitor– enzyme complexes or given for the complex leading to the highest binding affinity (see text)

| Averaged binding affinity | | | | | | Highest binding affinity | | | | |
|---|---|---|---|---|---|---|---|---|---|---|
| Compound | $\Delta G_{int}$ | $\Delta\Delta G_{s,L}$ | $\Delta G_{vdW}$ | $\sigma\Delta SAS_L$ | $\Delta\Delta G_{binding}$[a] | $\Delta G_{int}$ | $\Delta\Delta G_{s,L}$ | $\Delta G_{vdW}$ | $\sigma\Delta SAS_L$ | $\Delta\Delta G_{binding}$[a] |
| H1 | −39.2 | 24.3 | −50.8 | −2.4 | 0.0 | −43.1 | 22.1 | −51.7 | −2.4 | 0.0 |
| H4 | −40.2 | 25.7 | −50.4 | −2.5 | 0.7 | −48.9 | 24.9 | −50.0 | −2.5 | −1.4 |
| H5 | −45.4 | 26.2 | −52.6 | −2.6 | −6.3 | −55.1 | 26.6 | −51.9 | −2.6 | −7.9 |
| H6 | −40.7 | 24.6 | −53.8 | −2.6 | −4.4 | −44.7 | 24.6 | −54.2 | −2.6 | −1.8 |
| H11 | −45.0 | 25.9 | −54.8 | −2.6 | −8.4 | −52.8 | 28.4 | −55.9 | −2.6 | −7.6 |
| H13 | −42.7 | 25.5 | −55.3 | −2.7 | −7.1 | −45.1 | 24.4 | −55.9 | −2.6 | −4.1 |

[a] Values relative to those of compound H1

**Table 4.** Differences (relative to those of huprine H1) in binding free energy (kcal/mol) determined from experimental data and from calculations for the subset of huprines. The rank of compounds is given in *parentheses*

| Compound | $\Delta\Delta G_{(-)}$ | $\Delta\Delta G_{(rac)}$ | MD/TI[a] | Eq. (8) | PB (aba) [b] | PB (hba) [b] |
|---|---|---|---|---|---|---|
| H1 | 0.0 (1) | 0.0 (1) | 0.0 (1) | 0.1 (1) | 0.0 (2) | 0.0 (1) |
| H6 | −0.3 (2) | −0.3 (2) | −0.5 (2) | −0.5 (2) | −4.4 (3) | −1.8 (3) |
| H11 | −1.2 (3) | −1.3 (3) | −3.5 (4) | −1.4 (3) | −8.4 (6) | −7.6 (5) |
| H4 | −1.5 (4) | −1.2 (4) | −2.6 (3) | −1.7 (5) | 0.7 (1) | −1.4 (2) |
| H13 | −2.1 (5) | −1.9 (6) | −4.5 (6) | −2.2 (6) | −7.1 (5) | −4.2 (4) |
| H5 | −2.2 (6) | −1.6 (5) | −3.8 (5) | −1.5 (4) | −6.3 (4) | −7.9 (6) |
| $r_S$[b] | | | 0.89[c] | 0.83[c] | 0.31 | 0.71 |

[a] Results obtained by averaging over the 20 structures collected from the molecular dynamics (*MD*) simulation (aba) or corresponding to the structure leading to the highest binding affinity (hba). Values taken from thermodynamic integration (*TI*) calculations reported in Refs. [15, 16]
[b] Root-mean-square deviation (kcal/mol) between experimental [data taken for the activity of the (−)-enantiomer] and predicted binding free energies. $r_S$: Spearman's correlation coefficient between experimental and predicted rank orders
[c] $p < 0.05$

electrostatic difference between bound and unbound states of the inhibitor does. The root-mean-square deviation (rmsd) between experimental and predicted (from Eq. 8) relative binding free energies is 0.3 kcal/mol. Indeed, the rank of predicted binding affinities reflects satisfactorily the ordering of experimental inhibitory potencies ($r_S = 0.83$). On the other hand, no significant correlation was found between the experimental binding free energies and either the van der Waals interaction energy or the change in the SAS.

$$\Delta\Delta G_{(-)} = 0.089\Delta\Delta U_{ele} + 0.08 \quad (8)$$

$$\Delta\Delta G_{(rac)} = 0.075\Delta\Delta U_{ele} + 0.04 \quad (9)$$

Table 4 also reports the relative binding free energies determined from PB/SA calculations. The rank ordering does not reproduce satisfactorily the experimental ordering of binding affinities when the binding free energies are determined by averaging over the ensemble of structures collected from the MD simulation ($r_S = 0.31$). Nevertheless, an improvement is observed when comparison is made using the highest binding affinities determined for this subset of huprines ($r_S = 0.71$).

The preceding results shows that the most rigorous method, i.e. MD/TI calculations, provides a reliable description of the rank ordering and even of the differences in binding affinities for the subset of compounds. This is, however, achieved at the expense of intensive computer calculations, which makes it desirable to resort to approximate methods for predicting relative binding affinities. Among the two procedures examined here, the MD/LR method performs better than PB/SA calculations to predict the differences in inhibitory potency. Moreover, the marked difference in the rank ordering predicted from the average binding affinities or the highest binding affinity in PB/SA calculations stresses the importance of selecting a proper structure of the inhibitor–enzyme complex.

In contrast to the MD/LR results, consideration of the differences in the PB electrostatic term alone between inhibitors (Eq. 6) was not useful to predict the rank of inhibitory potencies. To investigate if this behavior was due to the approximate procedure described in the Methods, we recomputed the PB electrostatic energies, considering explicitly the desolvation of the enzyme

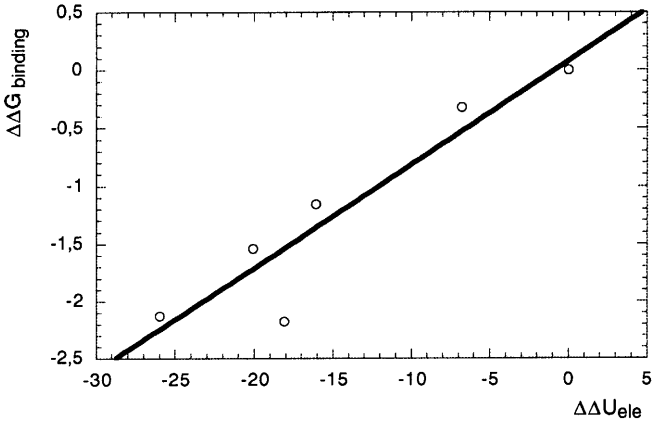


**Fig. 2.** Representation of the relative free energy of binding for the (−)-enantiomer of the huprine series versus the electrostatic contribution in the molecular dynamics/linear response approximation

**Table 5.** Differences [relative to those of huprine H1, results obtained by averaging over the 20 structures collected from the MD simulation (aba) or corresponding to the structure leading to the highest binding affinity (hba)] (kcal/mol) in experimental binding free energy and the electrostatic binding free energy determined from PB calculations for the subset of huprines. The rank of the compounds is given in parentheses

| Compound | $\Delta\Delta G_{(-)}$ | Eq. (6) (aba) | Eq. (6) (hba) | Eq. (5) (aba) | Eq. (5) (hba) |
|---|---|---|---|---|---|
| H1 | 0.0 (1) | 0.0 (2) | 0.0 (3) | 0.0 (1) | 0.0 (1) |
| H6 | −0.3 (2) | −1.2 (3) | 0.9 (1) | −0.3 (2) | −2.8 (3) |
| H11 | −1.2 (3) | −4.2 (5) | −3.4 (5) | −1.8 (5) | −3.3 (5) |
| H4 | −1.5 (4) | 0.4 (1) | −3.0 (4) | −0.8 (3) | −2.9 (4) |
| H13 | −2.1 (5) | −2.3 (4) | 0.3 (2) | −1.7 (4) | −1.9 (2) |
| H5 | −2.2 (6) | −4.3 (6) | −7.5 (6) | −2.0 (6) | −4.6 (6) |
| $R_s$[a] | | 0.54 | 0.49 | 0.83[b] | 0.60 |

[a] Spearman's correlation coefficient between experimental and predicted rank orders
[b] $p < 0.05$

(Eq. 5), and a focusing technique was also employed to reach a final grid step of 0.8 Å/point. Inspection of the results in Table 5 shows that, compared to the experimental ordering of binding affinities, the rank of the

compounds is now better, especially when the average values are considered. These results point out the need to reduce errors associated with the grid in finite-difference calculations. Nevertheless, there are still differences in the rank ordering of the compounds depending on whether the results computed from the ensemble average or from the complex structure leading to the highest binding affinity are considered. This illustrates the sensitivity of PB calculations to the particular configuration adopted for the inhibitor–enzyme complex. Accordingly, the intrinsic approximations of the PB continuum treatment do not seem to be adequate when one has to discriminate between compounds with inhibitory potencies lying in a narrow range. In this case, the use of methods relying on an explicit structural description of the inhibitor–receptor complex seems to be necessary.

Let us know extend this investigation to the complete series of huprine derivatives, which involve different substituents and substitution patterns, though the range of inhibitory activity remains unchanged. To this end, the activity of those compounds with unknown IC50 values for the bioactive enantiomer was estimated from the IC50 data determined for the racemic mixture (see Methods). Owing to the limited accuracy of PB/SA calculations (see earlier), this analysis was performed only using the MD/LR results, which are given in Table 6.

The predictive power of Eq. (8) for the whole series of huprines is not as good as for the subset of compounds. Thus, the rmsd between experimental and predicted binding affinities amounts to 1.4 kcal/mol and, regarding the rank of the huprines, Spearman's correlation coefficient is 0.66. As expected, a reparameterization of the extended linear model is necessary owing to the larger chemical diversity of the complete series of huprines. The electrostatic term still exhibits the largest correlation with the experimental data, leading to the regression equation noted in Eq. (10) ($p < 0.05$). The regression coefficient is still positive, but is smaller than that in Eq. (8). Pearson's correlation coefficient (0.58) is also smaller than for the previous subset of compounds; however, both the rmsd between experimental and predicted binding free energies (0.6 kcal/mol) and Spearman's correlation coefficient (0.74) improve compared to the values obtained when Eq. (8) is used directly (see earlier and Table 6).

$$\Delta\Delta G_{(-)} = 0.024\Delta\Delta U_{\mathrm{ele}} - 0.57 \tag{10}$$

Reparameterization of Eq. (10) to include other contributions led to the regression equation noted in Eq. (11), which was found to be statistically significant with a confidence level of 95%. Compared to Eq. (10), Eq. (11) reduces the rmsd between experimental and predicted binding affinities to 0.5 kcal/mol and improves the rank of the compounds ($r_S = 0.83$). Indeed, the group of compounds with the highest inhibitory potency is correctly identified.

$$\Delta\Delta G_{(-)} = -0.557\Delta\Delta U_{\mathrm{vdW}} + 0.019\Delta\Delta U_{\mathrm{ele}} + 0.034\Delta\Delta\mathrm{SAS} - 0.18 \tag{11}$$

Looking at the adjustable parameters, the coefficients of the electrostatic and SAS terms are positive. However, the coefficient of the van der Waals component ($\alpha$) is negative, which means that a better van der Waals interaction with the enzyme decreases the inhibitory potency. This finding seemed unreasonable, though it might imply some kind of steric collapse of either the inhibitor or the protein; however, the changes in the internal energy do not support this possibility. Since the $\Delta\Delta U_{\mathrm{vdW}}$ and $\Delta\Delta$SAS terms are highly correlated ($r_P = 0.91$, $p < 0.001$), their role in Eq. (10) probably reflects a spurious cancellation of contributions that increase the correlation with the fitted data. The uncertainties in the (ensemble-averaged) energetic terms and in the experimental measures makes it difficult to establish a chemically significant relationship able to explain the small differences in binding affinities for the complete series of huprines.

## 4 Conclusion

Methods based on the LR approximation provide detailed information on the (ensemble-averaged) inter-

**Table 6.** Averaged electrostatic and van der Waals interaction energies (kcal/mol) and SAS (Å$^2$) for the inhibitor complexed to the enzyme and in solution

| Compound | Van der Waals | | | Electrostatic | | | SAS | | |
|---|---|---|---|---|---|---|---|---|---|
| | $U_{\mathrm{bound}}$ | $U_{\mathrm{unbound}}$ | $\Delta\Delta U_{\mathrm{vdW}}$[a] | $U_{\mathrm{bound}}$ | $U_{\mathrm{unbound}}$ | $\Delta\Delta U_{\mathrm{ele}}$[a] | Bound | Unbound | $\Delta\Delta$SAS[a] |
| H1 | −48.0 | −23.7 | 0.0 | −164.9 | −75.2 | 0.0 | 18.2 | 449.2 | 0.0 |
| H2 | −51.4 | −25.6 | −1.5 | −208.7 | −73.4 | −45.6 | 14.1 | 482.7 | −37.6 |
| H3 | −49.0 | −24.8 | 0.1 | −160.2 | −72.4 | 1.9 | 21.9 | 449.5 | 3.4 |
| H4 | −47.7 | −24.2 | 0.8 | −189.1 | −79.3 | −20.1 | 16.1 | 460.7 | −13.5 |
| H5 | −48.9 | −24.8 | 0.2 | −186.8 | −79.0 | −18.1 | 13.4 | 474.1 | −29.7 |
| H6 | −49.8 | −24.8 | −0.7 | −172.1 | −75.6 | −6.8 | 14.1 | 473.1 | −28.0 |
| H7 | −54.0 | −27.3 | −2.4 | −176.4 | −71.1 | −15.6 | 16.2 | 493.1 | −45.9 |
| H8 | −54.2 | −26.6 | −3.3 | −213.4 | −73.9 | −49.8 | 13.8 | 506.8 | −61.9 |
| H9 | −57.3 | −28.9 | −4.1 | −207.7 | −70.0 | −48.1 | 16.9 | 530.9 | −82.9 |
| H10 | −51.2 | −25.7 | −1.2 | −160.4 | −74.5 | 3.7 | 17.1 | 479.5 | −31.4 |
| H11 | −51.2 | −25.3 | −1.6 | −184.1 | −78.4 | −16.1 | 13.4 | 485.0 | −40.6 |
| H12 | −52.6 | −25.8 | −2.5 | −159.8 | −73.6 | 3.5 | 14.4 | 492.7 | −47.3 |
| H13 | −52.0 | −25.6 | −2.1 | −194.0 | −78.3 | −26.0 | 13.6 | 504.2 | −59.6 |
| H14 | −54.0 | −27.2 | −2.5 | −184.8 | −75.1 | −20.0 | 25.2 | 522.8 | −66.6 |

[a] Values relative to those of compound H1

**Table 7.** Relative differences (relative to those of huprine H1) in binding free energy (kcal/mol) determined from the experimental IC50 data of the racemic mixture and from MD/linear response calculations for the huprine derivatives. The rank of compounds is given in *parentheses*

| Compound | $\Delta\Delta G_{(rac)}$ | Eq. (10) | Eq. (11) |
|---|---|---|---|
| H1 | 0.0 (1) | −0.6 (4) | −0.2 (2) |
| H10 | −0.2 (2) | −0.5 (1) | −0.5 (4) |
| H6 | −0.3 (3) | −0.7 (5) | −0.9 (6) |
| H14 | −0.3 (4) | −1.0 (7) | −1.4 (8) |
| H7 | −0.3 (5) | −0.9 (6) | −0.7 (5) |
| H3 | −0.5 (6) | −0.5 (2) | −0.1 (1) |
| H12 | −0.9 (7) | −0.5 (3) | −0.3 (3) |
| H2 | −1.1 (8) | −1.7 (12) | −1.5 (10) |
| H8 | −1.1 (9) | −1.8 (14) | −1.4 (9) |
| H11 | −1.3 (10) | −1.0 (8) | −1.0 (7) |
| H4 | −1.5 (11) | −1.1 (10) | −1.5 (11) |
| H13 | −2.1 (12) | −1.2 (11) | −1.5 (12) |
| H5 | −2.2 (13) | −1.0 (9) | −1.6 (13) |
| H9 | −2.3 (14) | −1.7 (13) | −1.6 (14) |
| $R_s$[a] | | 0.74[b] | 0.83[b] |

[a] Root-mean-square deviation (kcal/mol) between experimental and predicted binding free energies. $r_S$: Spearman's correlation coefficient between experimental and predicted rank orders
[b] $p < 0.01$

action energy of the inhibitor with its surroundings. The success of these methods, nevertheless, can be restricted by the accuracy of the force field and the limited sampling of the system. On the other hand, PB/SA calculations offer a complementary approach that replaces the microscopic description of the solvent by a continuum. PB/SA calculations are generally performed using a single structure of the inhibitor–enzyme complex, which may make difficult the identification of the various local minima for the binding of the drug. These difficulties can be alleviated by resorting to the calculation for an ensemble of equilibrated configurations of the system. However, these calculations involve an estimation of solvation free energies of macromolecular systems, which are subject to large numerical errors.

For the particular series of huprine derivatives examined here, MD/LR results provide a better description of the ordering of inhibitory potencies than PB/SA calculations. This is largely motivated by the small range of binding affinities of the available huprines, which demands a more detailed structural description of the interaction of the inhibitor with its environment. However, its accuracy is also sensitive to the range of binding affinities of the compounds under study. Clearly, free-energy calculations appear to be the only reliable procedure to discriminate between compounds with small differences (1–2 kcal/mol) in inhibitory potencies. Otherwise, both LR and PB/SA calculations should be restricted to series of compounds covering a wider range of inhibitory potencies (greater than 2 kcal/mol). Thus, the combination of PB/SA calculations as a preliminary step followed by LR studies as a confirmatory step could be valuable to identify potentially active compounds in lead optimization and screening of chemical libraries.

*Acknowledgements*. We are grateful to J.L. Sussman for sending us the crystallographic data of the huprine–AChE complex prior to publication. We also thank the Fundació La Marató de TV3 (project 3004/97) and the Dirección General de Investigación Científica y Técnica (project PB98-1222) for financial support, and the Centre de Supercomputació de Catalunya (CESCA) for computational facilities. A fellowship from the Ministerio de Educación y Cultura to X.B. is kindly acknowledged.

## References

1. Benzi G, Moretti A (1998) Eur J Pharmacol 346: 1–13
2. Brufani M, Filocamo L, Lappa S, Maggi A (1997) Drugs Future 22: 397
3. (1987) Drugs Future 12: 1032
4. (a) Kozikowski A P, Xia Y, Reddy ER, Tückmantel W, Hanin I, Tang XC (1991) J Org Chem 56: 4636; (b) Kozikowski AP, Campini G, Sun LQ, Wang S, Saxena A, Doctor BP (1996) J Am Chem Soc 118: 11357; (c) Kozikowski AP, Ding Q, Saxena A, Doctor BP (1996) Bioorg Med Chem Lett 6: 259; (d) Kaneko S, Nakajima N, Shikano M, Katoh T, Terashima S (1998) Tetrahedron 54: 5485
5. (a) Pang YP, Quiram P, Jelacic T, Hong F, Brimijoin SJ (1996) Biol Chem 271: 23646; (b) Jaen JC, Gregor VE, Lee C, Davis R, Emmerling M (1996) Bioorg Med Chem Lett 6: 737
6. (a) Chen YL, Nielsen J, Medberg K, Dunaiskis A, Jones S, Russo L, Johnson J, Ives J, Liston DJ (1992) Med Chem 35: 1429; (b) Atack JR, Yu QS, Soncrant TT, Brossi A, Rapoport SJ (1998) Pharmacol Exp Ther 249: 194
7. Villalobos A, Butler TW, Chapin DS, Chen YL, DeMattos SB, Ives JL, Jones SB, Liston DR, Nagel AA, Nason DM, Nielsen JA, Ramirez AD, Shalaby IA, White WF (1995) J Med Chem 38: 2802
8. Rampa A, Bisi A, Valenti P, Recanatini M, Cavalli A, Andrisano V, Cavrini V, Fin L, Buriani A, Giusti PJ (1998) Med Chem 41: 3976
9. Sugimoto H, Iimura Y, Yamanishi Y, Yamatsu KJ (1995) Med Chem 38: 4821
10. Prous J, Rabasseda X, Castañer J (1996) Drugs Future 10: 656
11. Aguado F, Badia A, Baños JE, Bosch F, Bozzo C, Camps P, Contreras J, Dierssen M, Escolano C, Görbig DM, Muñoz-Torrero D, Pujol MD, Simon M, Vázquez MT, Vivas NM (1994) Eur J Med Chem 29: 205
12. Badia A, Baños JE, Camps P, Contreras J, Görbig DM, Muñoz-Torrero D, Simon M, Vivas NM (1998) Bioorg Med Chem 6: 427
13. Camps P, El Achab R, Görbig DM, Morral J, Muñoz-Torrero D, Badia A, Baños JE, Vivas NM, Barril X, Orozco M, Luque FJ (1999) J Med Chem 42: 3227
14. Camps P, Cusack B, Mallender WD, El Achab R, Morral J, Muñoz-Torrero D, Rosenberry TL (2000) Mol Pharmacol 57: 409
15. Camps P, El Achab R, Morral J, Muñoz-Torrero D, Badia A, Baños JE, Vivas NM; Barril X, Orozco M, Luque FJ (2000) J Med Chem (in press)
16. Barril X, Orozco M, Luque FJ (1999) J Med Chem 42: 5110
17. Harel M, Schalk I, Ehret-Sabatier L, Bouet F, Goeldner M, Hirth C, Axelsen P, Silman I, Sussman JL (1993) Proc Natl Acad Sci USA 90: 9031
18. Raves ML, Harel M, Pang YP, Silman I, Kozikowski AP, Sussman JL (1997) Nature Struct Biol 4: 57
19. Kollamn P (1993) Chem Rev 93: 2395
20. (a) Åqvist J, Medina C, Samuelsson JE (1994) Protein Eng 7: 385; (b) Hansson T, Åqvist J (1995) Protein Eng 8: 1137; (c) Åqvist J (1996) J Comput Chem 17: 1587
21. (a) McDonald NA, Carlson HA, Jorgensen WL (1997) J Phys Org Chem 10: 563; (b) Smith RH Jr, Jorgensen WL, Tirado-Rives J, Lamb ML, Janssen PAJ, Michejda CJ, Smith MBK (1998) J Med Chem 41: 5272

22. (a) Hansson T, Marelius J, Aqvist J (1998) J Comput-Aided Mol Des 12: 27; (b) Jones-Hertzog DK, Jorgensen WL (1997) J Med Chem 40: 1539
23. (a) Gilson MK, Honig B (1988) Proteins Struct Funct Genet 4: 7; (b) Gilson MK, Sharp KA, Honig BH (1988) J Comput Chem 9: 327; (c) Sharp KA, Honig B (1990) Annu Rev Biophys Biophys Chem 19: 301
24. Pitera J, Kollman P (1998) J Am Chem Soc 120: 7557
25. Radmer RJ, Kollman PA (1998) J Comput-Aided Mol Des 12: 215
26. Jorgensen WL, Chandrasekhar J, Madura JD, Impey RW, Klein ML (1983) J Chem Phys 79: 926
27. Wlodek ST, Antosiewicz J, McCammon JA, Straatsma TP, Gilson MK, Briggs JM, Humblet C, Sussman JL (1996) Biopolymers 38: 109
28. Hariharan PC, Pople JA (1973) Theor Chim Acta 28: 213
29. Frisch MJ, Trucks GW, Schlegel HB, Gill PMW, Johnson BG, Robb MA, Cheeseman JR, Keith TA, Petersson GA, Montgomery JA, Raghavachari K, Al-Laham MA, Zakrzewski VG, Ortiz JV, Foresman JB, Cioslowski J, Stefanov BB, Nanayakkara A, Challacombe M, Peng CY, Ayala PY, Chen W, Wong MW, Andres JL, Replogle ES, Gomperts R, Martin RL, Fox DJ, Binkley JS, Defrees DJ, Baker J, Stewart JP, Head-Gordon M, Gonzalez C, Pople JA (1995) Gaussian 94, revision A1. Gaussian, Pittsburgh, Pa
30. Cornell WD, Cieplak P, Bayly CI, Gould IR, Merz K, Ferguson DM, Spellmeyer DC, Fox T, Caldwell JW, Kollman PA (1995) J Am Chem Soc 117: 5179
31. Bayly CI, Cieplak P, Cornell WD, Kollman PA (1993) J Chem Phys 97: 10269
32. Ryckaert JP, Ciccotti G, Berendsen HJC (1977) J Comput Phys 23: 327
33. Case DA, Pearlman DA, Caldwell JC, Cheatham TE, Ross WS, Simmerling C, Darden T, Merz KM, Stanton RV, Cheng A, Vincent JJ, Crowley M, Ferguson DM, Radmer R, Seibel GL, Singh UC, Weiner P, Kollman PA (1997) AMBER5. University of California: San Francisco
34. Gelpí JL, Luque FJ, Orozco M (2000) CMIP program. University of Barcelona
35. Sitkoff D, Sharp KA, Honig B (1994) J Phys Chem 98: 1978
36. Eriksson MAL, Pitera J, Kollman PA (1999) J Med Chem 42: 868